



## Journal of Advanced Research in Fluid Mechanics and Thermal Sciences

Journal homepage:  
[https://semarakilmu.com.my/journals/index.php/fluid\\_mechanics\\_thermal\\_sciences/index](https://semarakilmu.com.my/journals/index.php/fluid_mechanics_thermal_sciences/index)  
ISSN: 2289-7879



# Analysis of Solution Stability in $Al_2O_3-Cu/H_2O$ over a Stretching/Shrinking Wedge

Nurul Amira Zainal<sup>1,2,\*</sup>, Najiyah Safwa Khashi'ie<sup>1,2</sup>, Iskandar Waini<sup>2,3</sup>, Khairum Hamzah<sup>2,3</sup>, Sayed Kushairi Sayed Nordin<sup>1,2</sup>, Abdul Rahman Mohd Kasim<sup>4</sup>, Roslinda Nazar<sup>5</sup>, Ioan Pop<sup>6</sup>

- <sup>1</sup> Fakulti Teknologi dan Kejuruteraan Mekanikal, Universiti Teknikal Malaysia Melaka, Hang Tuah Jaya, 76100 Durian Tunggal, Melaka, Malaysia
- <sup>2</sup> Forecasting and Engineering Technology Analysis (FETA) Research Group, Universiti Teknikal Malaysia Melaka, Hang Tuah Jaya, 76100 Durian Tunggal, Melaka, Malaysia
- <sup>3</sup> Fakulti Teknologi dan Kejuruteraan Industri dan Pembuatan, Universiti Teknikal Malaysia Melaka, Hang Tuah Jaya, 76100 Durian Tunggal, Melaka, Malaysia
- <sup>4</sup> Pusat Sains Matematik, Universiti Malaysia Pahang, Lebuhraya Persiaran Tun Khalil Yaakob, 26300 Kuantan, Pahang, Malaysia
- <sup>5</sup> Department of Mathematical Sciences, Faculty of Science and Technology, Universiti Kebangsaan Malaysia, 43600 Bangi Selangor, Malaysia
- <sup>6</sup> Department of Mathematics, Babes-Bolyai University, Cluj-Napoca, Romania

### ARTICLE INFO

### ABSTRACT

#### Article history:

Received 19 August 2023  
Received in revised form 29 October 2023  
Accepted 11 November 2023  
Available online 30 November 2023

#### Keywords:

Stability analysis; hybrid nanofluids; wedge; heat source; MHD

In this study, the stability analysis is conducted in order to observe the reliability of the generated solutions. The influence of several parameters is taken into consideration including heat source/sink parameter, suction, magnetic field, and heat transfer. The well-known heat transfer fluid that is  $Al_2O_3-Cu/H_2O$  hybrid nanofluid past a stretching/shrinking wedge is implied. The similarity equations are achieved after implying suitable similarity transformation which then needed to be solved numerically using *bvp4c*, embedded in MATLAB software. Dual solutions are observed along the investigation within specified values of involved parameters. It is important to note that verification results show excellent concordance with pre-existing reports.

## 1. Introduction

Hybrid nanofluids have been created recently to enhance the fluids' thermophysical and heat-transporting capabilities. Even so, one of the most important factors in preserving a stable hybrid nanofluid composition is picking the appropriate nanoparticles. Therefore, exploring the full potential of this powerful nanofluid mixture requires continual investigation. Numerous studies have lately focused on the efficiency of hybrid nanofluids as heat-transfer fluids in a variety of flows and surfaces, including wedge-shaped surfaces. This is noteworthy due to the several uses in the chemical and technical fields, including those related to geothermal energy and aerodynamics [1,2]. Zainal *et al.*, [3] and Rehman *et al.*, [4] claimed that selecting different and appropriate nanoparticle proportions in the hybrid nanofluids through a wedge will enable one to achieve the necessary heat transfer rate.

\* Corresponding author.

E-mail address: [nurulamira@utem.edu.my](mailto:nurulamira@utem.edu.my)

<https://doi.org/10.37934/arfmts.111.2.116125>

Additional promising discoveries about how hybrid nanofluids could improve heat transfer are available in Sajjad *et al.*, [5] and Idris *et al.*, [6]. Thus, in accordance with the literature mentioned above, this suggests that hybrid nanofluids could speed up the heating process of the stretching/shrinking wedge.

The implications of heat source/sink should not be ignored because the majority of engineering operations usually entail extremely high temperatures. Since the heat source/sink parameter contributes to the trend of boundary layer temperature, which in turn impacts product quality, the investigation of heat source/sink is crucial in boundary layer flows and heat transfer. When the heat source/sink parameters are included in the fluid flows study, Manohar *et al.*, [7] found that the temperature of the hybrid nanofluids is invariably higher than the temperature of the nanofluids. In another study, Masood *et al.*, [8] concluded that the temperature field increases for the heat source/sink factor while the velocity field is boosted for the velocity ratio parameter. The analytical and numerical analysis of heat transfer and boundary layer flow with a focus on the heat source/sink parameter in the hybrid nanofluid is available in previous researches [9-11].

The goal of the current work is to fill a knowledge gap, notably in the area of hybrid nanofluid flow with the effects of heat source/sink on a stretching/shrinking wedge surface. The main contribution of this study is the development of a new mathematical hybrid nanofluids model with the inclusion of the heat source/sink parameter, which also witnessed the appearance of several other significant variables like the magnetic field and suction effect. This study also noted the establishment of numerous solutions. Given the considerable relevance practical of the boundary layer flow behavior of the wedge-shaped surface, this important discovery could contribute to a better knowledge of this research.

## 2. Methodology

A steady magnetohydrodynamics (MHD)  $\text{Al}_2\text{O}_3\text{-Cu}/\text{H}_2\text{O}$  hybrid nanofluids flow with the effect of heat source/sink over a stretching/shrinking wedge is studied which shown in Figure 1. The free-stream velocity is given by  $u_e = U_e x^m$  with  $u_w(x) = U_w x^m$  is the velocity of the stretching/shrinking wedge. Next,  $U_e$  is a constant,  $U_w > 0$  and  $U_w < 0$  denote as the stretching wedge and shrinking wedge, respectively. Further, we have  $m = \beta/(2 - \beta)$  where  $m$  represents angle of the wedge and  $\beta$  is the Hartree pressure gradient parameters. Since the wedge flow problem is measured in this study, thus the value of  $m$  is set in the range of  $0 < m < 1$ . To be exact, the value of  $m$  is set to 0.1 which represents the acute wedge angle. The fluid's ambient temperature is represented by the stretching/shrinking wedge temperature, where both temperatures are set to be constant. A magnetic field  $B(x)$  is applied in the  $y$ - direction with  $B(x) = B_0 x^{(m-1)/2}$  where  $B_0$  is the applied magnetics field strength.

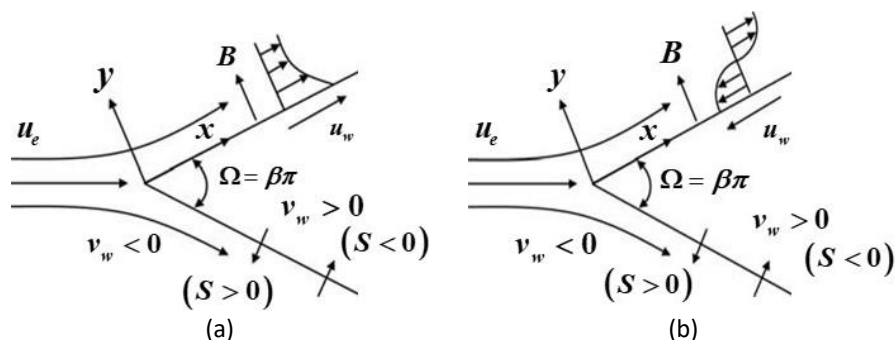


**Fig. 1.** The coordinate systems for (a) stretching wedge (b) shrinking wedge

Based on the above assumption, the governing equations of the hybrid nanofluids mathematical model can be written as [12,13]:

$$\frac{\partial u}{\partial x} + \frac{\partial v}{\partial y} = 0, \quad (1)$$

$$u \frac{\partial u}{\partial x} + v \frac{\partial u}{\partial y} = u_e \frac{du_e}{dx} + \frac{\mu_{hnf}}{\rho_{hnf}} \frac{\partial^2 u}{\partial y^2} - \frac{\sigma_{hnf}}{\rho_{hnf}} B^2 (u - u_e), \quad (2)$$

$$u \frac{\partial T}{\partial x} + v \frac{\partial T}{\partial y} = \frac{k_{hnf}}{(\rho C_p)_{hnf}} \frac{\partial^2 T}{\partial y^2} - \frac{Q_0}{(\rho C_p)_{hnf}} (T - T_\infty). \quad (3)$$

Meanwhile, the boundary conditions of the above mathematical assumption are given as follows

$$\begin{aligned} v = v_w(x), u = u_w(x), T = T_w, \quad \text{at } y = 0, \\ u \rightarrow u_e(x), T \rightarrow T_\infty(x), \quad \text{as } y \rightarrow \infty. \end{aligned} \quad (4)$$

The heat source/sink variable is denoted as  $Q_0 = Q^* u_e x^{(m-1)}$  with constant  $Q^*$ . The thermophysical characteristic of related fluids are portrayed in Table 1 while the correlation coefficient for the hybrid nanofluids is depicted in Table 2. The following similarity variables are now presented [12]

$$\psi = (U_e \nu_f)^{1/2} x^{(m+1)/2} f(\eta), \quad \eta = (U_e / \nu_f)^{1/2} x^{(m-1)/2} f(\eta) y, \quad \theta(\eta) = \frac{T - T_\infty}{T_w - T_\infty}, \quad (5)$$

thus,

$$v_w = -\frac{m+1}{2} (U_e \nu_f)^{1/2} x^{(m-1)/2} S. \quad (6)$$

**Table 1**

Properties of the base fluid and nanoparticles [14]

Component	$\rho$ (kg/m <sup>3</sup> )	$k$ (W / mK)	$C_p$ (J/kgK)
Al <sub>2</sub> O <sub>3</sub>	3970	40	765
H <sub>2</sub> O	0.613	21	4179
Cu	8933	400	385

**Table 2**

Nanofluids with hybrid thermal properties [15]

Thermophysical properties	Alumina-Copper/Water (Al <sub>2</sub> O <sub>3</sub> -Cu/H <sub>2</sub> O)
Thermal conductivity, $k_{hnf}$	$\frac{k_{hnf}}{k_f} = \left[ \frac{\left( \frac{\phi_1 k_{Al_2O_3} + \phi_2 k_{Cu}}{\phi_{hnf}} \right) + 2k_f + 2(\phi_1 k_{Al_2O_3} + \phi_2 k_{Cu}) - 2\phi_{hnf} k_f}{\left( \frac{\phi_1 k_{Al_2O_3} + \phi_2 k_{Cu}}{\phi_{hnf}} \right) + 2k_f - (\phi_1 k_{Al_2O_3} + \phi_2 k_{Cu}) + \phi_{hnf} k_f} \right]$
Heat capacity, $(\rho C_p)_{hnf}$	$(\rho C_p)_{hnf} - (1 - \phi_{hnf})(\rho C_p)_f = \phi_1 (\rho C_p)_{Al_2O_3} + \phi_2 (\rho C_p)_{Cu}$
Electrical conductivity, $\sigma_{hnf}$	$\frac{\sigma_{hnf}}{\sigma_f} = \left[ \frac{\left( \frac{\phi_1 \sigma_{Al_2O_3} + \phi_2 \sigma_{Cu}}{\phi_{hnf}} \right) + 2\sigma_f + 2(\phi_1 \sigma_{Al_2O_3} + \phi_2 \sigma_{Cu}) - 2\phi_{hnf} \sigma_f}{\left( \frac{\phi_1 \sigma_{Al_2O_3} + \phi_2 \sigma_{Cu}}{\phi_{hnf}} \right) + 2\sigma_f - (\phi_1 \sigma_{Al_2O_3} + \phi_2 \sigma_{Cu}) + \phi_{hnf} \sigma_f} \right]$

For further details,  $S$  in the Eq. (6) is the parameter of mass flux and in this study, we only considered the positive values where  $S > 0$  which represents the suction parameter. The following ordinary (similarity) differential equations are then developed by utilising the similarity variables in Eq. (5) and Eq. (6) thus

$$\frac{\mu_{hnf}/\mu_f}{\rho_{hnf}/\rho_f} f''' + \frac{m+1}{2} f f'' + m(1-f'^2) - \frac{\sigma_{hnf}/\sigma_f}{\rho_{hnf}/\rho_f} M(f'-1) = 0, \quad (7)$$

$$\frac{1}{Pr} \left( \frac{k_{hnf}/k_f}{(\rho C_p)_{hnf}/(\rho C_p)_f} \right) \theta'' + \frac{m+1}{2} f \theta' + \frac{H}{(\rho C_p)_{hnf}/(\rho C_p)_f} \theta = 0, \quad (8)$$

$$\begin{aligned} f(0) = S, \quad f'(0) = \lambda, \quad \theta(0) = 1, \\ f'(\eta) \rightarrow 1, \quad \theta(\eta) \rightarrow 0, \end{aligned} \quad (9)$$

where  $M = \sigma_f B_0^2 / \rho_f U_e$  is the magnetic coefficient,  $Pr = \nu_f / \alpha_f$  is the Prandtl number, and  $\lambda = U_w / U_e$  represents the stretching/shrinking wedge parameter. The heat source/sink parameter is denoted as  $H = Q^* / (\rho C_p)_f$ . The physical quantities related to this study is declared as

$$Nu_x = \frac{x k_{hnf}}{k_f (T_w - T_\infty)} \left( -\frac{\partial T}{\partial y} \right)_{y=0} \quad \text{and} \quad C_f = \frac{\mu_{hnf}}{\rho_f u_\infty^2} \left( \frac{\partial u}{\partial y} \right)_{y=0}. \quad \text{Then, we get}$$

$$\text{Re}_x^{1/2} C_f = \frac{\mu_{hmf}}{\mu_f} f''(0), \quad \text{Re}_x^{-1/2} Nu_x = -\frac{k_{hmf}}{k_f} \theta'(0), \quad (10)$$

where  $\text{Re}_x = u_e(x)x/\nu_f$ .

### 3. Stability Analysis

In this section, the stability analysis is conducted in order to verify the solution reliability since there are more than one solution in the obtained results. The following transformations are presented based on the work reported by Weidman *et al.*, [16], Harris *et al.*, [17] and Merkin [18]:

$$u = U_e x^m f'(\eta, \Phi), \quad v = -\frac{m+1}{2} (U_e \nu_f)^{1/2} x^{(m-1)/2} \left( f(\eta, \Phi) + \frac{m-1}{m+1} \eta f'(\eta, \Phi) \right), \quad (11)$$

$$\theta(\eta, \Phi) = \frac{T - T_\infty}{T_w - T_\infty}, \quad \eta = y (U_e / \nu_f)^{1/2} x^{(m-1)/2}, \quad \Phi = U_e x^{m-1} t.$$

By employing the new transformation in the above equation, now Eq. (7) to Eq. (9) are converting into

$$\frac{\mu_{hmf}/\mu_f}{\rho_{hmf}/\rho_f} \frac{\partial^3 f}{\partial \eta^3} + \frac{m+1}{2} f \frac{\partial^2 f}{\partial \eta^2} + m \left( 1 - \left( \frac{\partial f}{\partial \eta} \right)^2 \right) - \frac{\sigma_{hmf}/\sigma_f}{\rho_{hmf}/\rho_f} M \left( \frac{\partial f}{\partial \eta} - 1 \right) - \frac{\partial^2 f}{\partial \eta \partial \Phi} = 0, \quad (12)$$

$$\frac{1}{\text{Pr}} \left( \frac{k_{hmf}/k_f}{(\rho C_p)_{hmf}/(\rho C_p)_f} \right) \frac{\partial^2 \theta}{\partial \eta^2} + \frac{m+1}{2} f \frac{\partial \theta}{\partial \eta} + \frac{H}{(\rho C_p)_{hmf}/(\rho C_p)_f} \theta - \frac{\partial \theta}{\partial \Phi} = 0, \quad (13)$$

$$f(0, \Phi) = S, \quad \frac{\partial f}{\partial \eta}(0, \Phi) = \lambda, \quad \theta(0, \Phi) = 1, \quad (14)$$

$$\frac{\partial f}{\partial \eta}(0, \Phi) \rightarrow 1, \quad \theta(0, \Phi) \rightarrow 0, \quad \text{as } \eta \rightarrow \infty.$$

Next, we applied the perturbation functions described by Weidman *et al.*, [16] where it is given that

$$f(\eta, \Phi) = f_0(\eta) + e^{-\Omega \Phi} \Upsilon(\eta, \Phi), \quad (15)$$

$$\theta(\eta, \Phi) = \theta_0(\eta) + e^{-\Omega \Phi} \Lambda(\eta, \Phi),$$

where  $\Upsilon(\eta)$  and  $\Lambda(\eta)$  are relatively small as compared with  $f_0$  and  $\theta_0$  and the unknown eigenvalue is assigned by  $\Omega$ . Next, we substitute Eq. (15) into Eq. (12) and Eq. (13) which transformed the equations to the linear eigenvalue problem where

$$\frac{\mu_{hmf}/\mu_f}{\rho_{hmf}/\rho_f} \Upsilon''' + \frac{m+1}{2} (f_0 \Upsilon'' + f_0'' \Upsilon) - 2mf_0' \Upsilon' - \frac{\sigma_{hmf}/\sigma_f}{\rho_{hmf}/\rho_f} M \Upsilon' + \Omega \Upsilon = 0, \quad (16)$$

$$\frac{1}{Pr} \left( \frac{k_{hmf}/k_f}{(\rho C_p)_{hmf}/(\rho C_p)_f} \right) \Lambda'' + \frac{m+1}{2} (f_0 \Lambda' + \theta_0' \Upsilon) + \left( \frac{H}{(\rho C_p)_{hmf}/(\rho C_p)_f} + \Omega \right) \Lambda = 0, \quad (17)$$

$$\begin{aligned} \Upsilon(0) = 0, \quad \Upsilon'(0) = 0, \quad \Lambda(0) = 0, \\ \Upsilon'(\infty) \rightarrow 1, \quad \Lambda(\infty) \rightarrow 0, \quad \text{as } \eta \rightarrow \infty. \end{aligned} \quad (18)$$

Without losing generality, we fix the value of  $\Upsilon''(0)$  as  $\Upsilon''(0) = 1$  in the current study and derive the value of  $\Omega$  from the system of equations in Eq. (16) and Eq. (17) in addition to the boundary condition (18). According to Eq. (15), as time passes, the flow is in a stable state if  $\Omega$  is positive and for negative values of  $\Omega$ , the flow is said to be in a state of instability. Meanwhile, when  $\Omega$  approaches the critical value or bifurcation point, the values of  $\Omega$  tend to zero for both positive and negative sides.

#### 4. Results and Discussions

In this section, the results obtained is discussed thoroughly. The reliability of the results is examined with Sparrow *et al.*, [19] and Ishak *et al.*, [20], as accessible in Table 3. The authors found that the present findings are very much in line with previous investigations. As a result, we are confident that the intended computer model can accurately anticipate the behaviour of dynamic fluid flow.

The numerical calculations for different physical parameters used in this study are performed. A variety of  $\phi$  is implemented ( $0.00 \leq \phi_1, \phi_2 \leq 0.01$ ) to differentiate between the conventional heat transfer fluid and the hybrid nanofluids. Furthermore, a variety of controlling parameter values are defined to the preceding scope where the value of the wedge angle and suction parameter are fixed to  $m = 0.1$ , and  $S = 2.0$ , respectively, while the magnetic are set within  $0.0 \leq M \leq 0.05$  and the heat source/sink parameter is classified in the range of  $0.0 \leq H \leq 0.5$  to guarantee the compatible of the obtained solutions. It should be emphasised that, in order to achieve the desired result, the values of the supplied parameter should be utilised to generate an adequate result estimation.

**Table 3**

Approximation values of  $f''(0)$  by certain values of  $S$  when  $\lambda = M = H = \phi_1 = \phi_2 = 0$ , and  $Pr = m = 1$

$S$	Present result	Sparrow <i>et al.</i> , [19]	Ishak <i>et al.</i> , [20]
1.0	1.889313	-	1.8893
0.5	1.541752	-	1.5418
0.0	1.232589	1.2310	1.2326
-0.5	0.969231	0.9697	0.9692
-1.0	0.756576	0.7605	0.7566

Figure 2 describes the influence of nanoparticles concentration when  $\phi$  is varied as the wedge shrinks. When  $\phi_1 = 0.00, \phi_2 = 0.01$ , the alumina-water nanofluid ( $Al_2O_3/H_2O$ ) is formed, meanwhile  $\phi_1 = 0.01, \phi_2 = 0.00$  denoted the copper-water nanofluid ( $Cu/H_2O$ ) and the combination of

$\phi_1 = \phi_2 = 0.01$  produced the alumina-copper/water hybrid nanofluids ( $\text{Al}_2\text{O}_3 - \text{Cu}/\text{H}_2\text{O}$ ). The improvement in velocity profiles  $f'(\eta)$  for both solutions is displayed when the value of  $\phi$  improves over the shrinking wedge, as illustrated in Figure 2(a). According to the findings, the  $\text{Al}_2\text{O}_3 - \text{Cu}/\text{H}_2\text{O}$  displayed the dominant trend of  $f'(\eta)$ , followed by  $\text{Cu}/\text{H}_2\text{O}$  and  $\text{Al}_2\text{O}_3/\text{H}_2\text{O}$ . This phenomenon causes the boundary layer separation on the shrinking wedge to slow down as a result of the frictional drag that is being exerted upsurges in the  $\text{Al}_2\text{O}_3 - \text{Cu}/\text{H}_2\text{O}$ . The trend of the temperature distributions profile  $\theta(\eta)$  corresponds to the increment of  $\phi$  is accessible in Figure 2(b). In Figure 2(b), the first solution shows an increase of  $\theta(\eta)$  from conventional fluid to nanofluid and hybrid nanofluid. In common practice,  $\text{Al}_2\text{O}_3 - \text{Cu}/\text{H}_2\text{O}$  shows better performance in heat transfer efficiency, followed by  $\text{Cu}/\text{H}_2\text{O}$  and  $\text{Al}_2\text{O}_3/\text{H}_2\text{O}$ . Aluminum is inferior to copper in terms of processor cooling since copper has a better thermal conductivity. But due to its lower density as compared to copper, aluminium can radiate heat into the air more effectively.

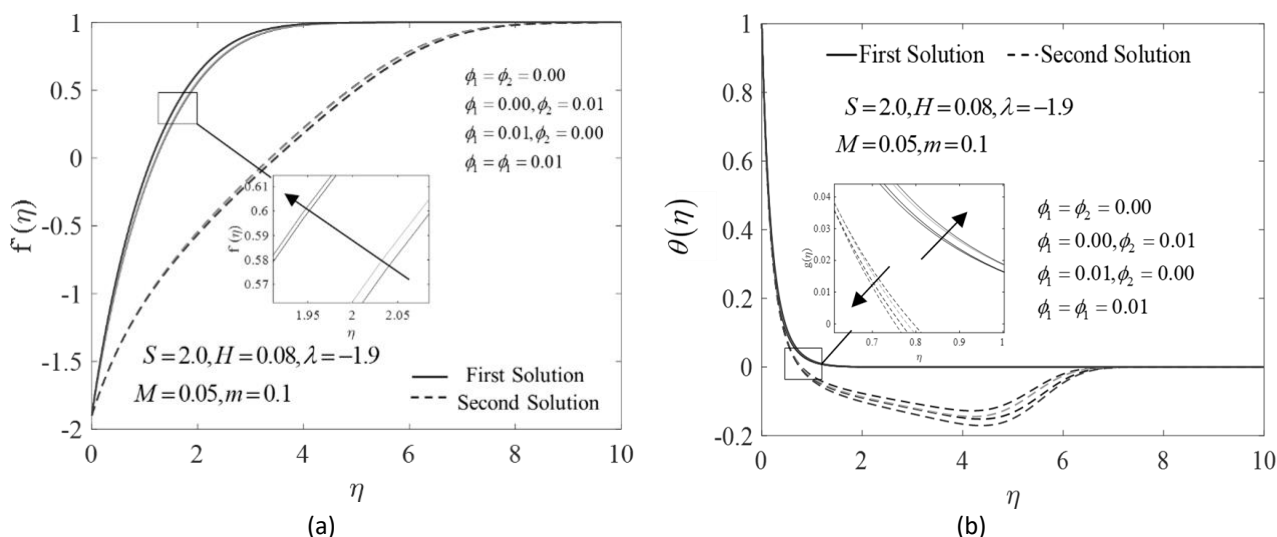
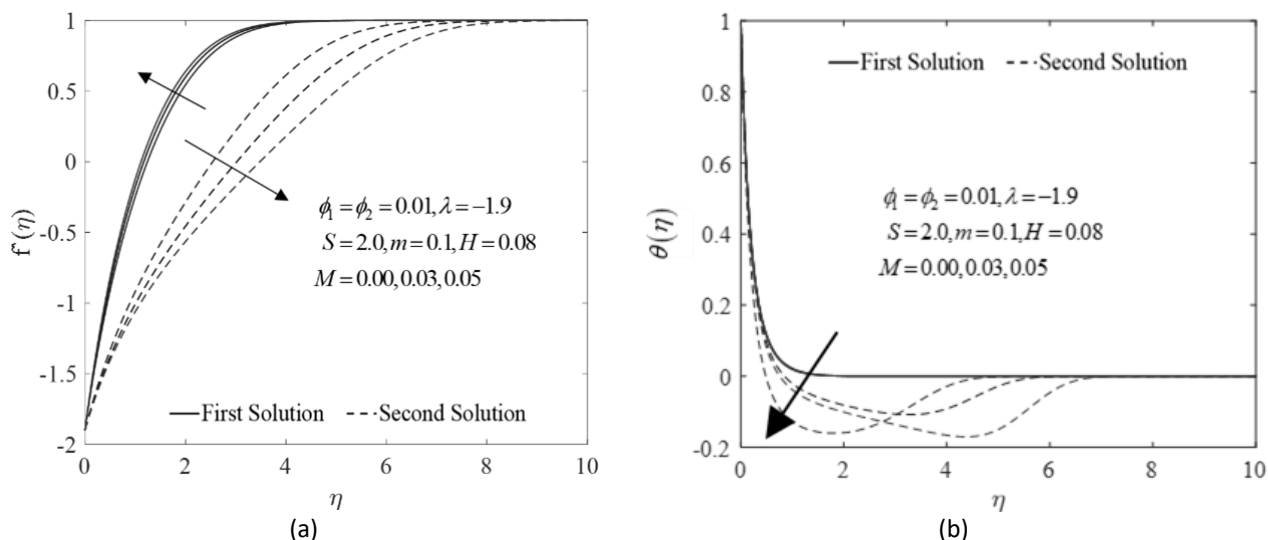
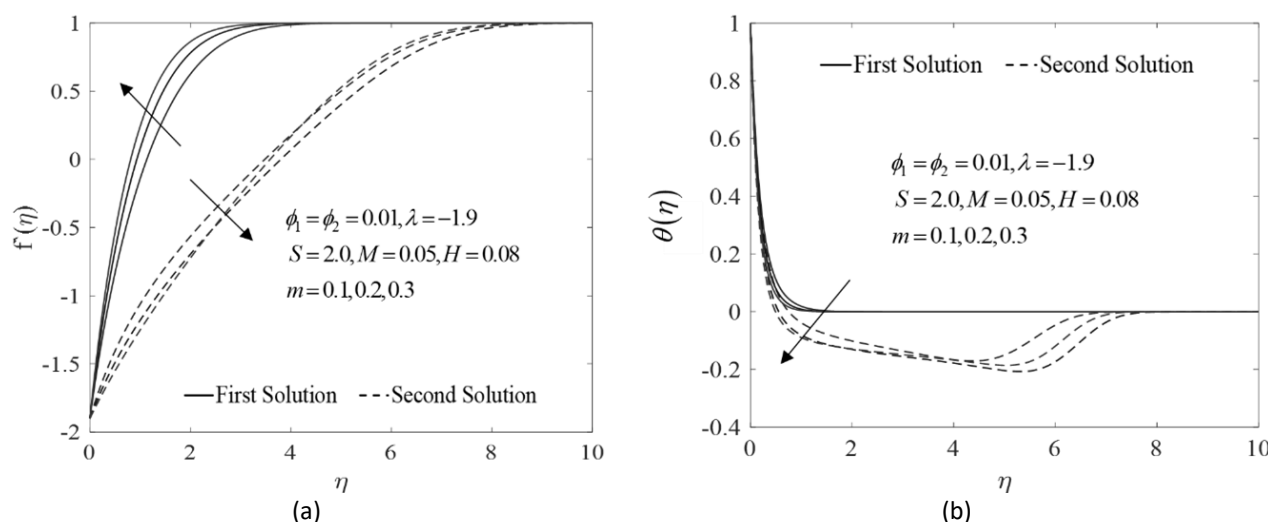


Fig. 2. Distribution profiles with different  $\phi$  in contrast to  $\eta$  (a) velocity profile (b) temperature profile

Figure 3(a) and Figure 3(b) depict the characteristics of  $f'(\eta)$  and  $\theta(\eta)$  with respect to the addition of magnetic parameter,  $M$ . Figure 3(a) apparently showed that the increasing values of  $M$  specifically in  $\text{Al}_2\text{O}_3 - \text{Cu}/\text{H}_2\text{O}$ , reduce the momentum boundary layer thickness in the first solution. However, the second solution showed the reduction trend as  $M$  increases. Meanwhile, it is observed that  $\theta(\eta)$  presents a downward trend in both solutions, as exhibited in Figure 3(b). As can be seen, the thickness of the thermal boundary layer declines in both profiles. The impact of wedge angle parameter,  $m$  in  $\text{Al}_2\text{O}_3 - \text{Cu}/\text{H}_2\text{O}$  are portrayed in Figure 4(a) and Figure 4(b) concerning  $f'(\eta)$  and  $\theta(\eta)$ , respectively. Figure 4(a) displays that as  $m$  improved,  $f'(\eta)$  increases in first solution, while the alternative solutions point out the opposite. On the other hand, Figure 4(b) illustrates a decreasing pattern of  $\theta(\eta)$  when  $m$  improves in first and second solutions, hence we can conclude that the thermal performance has progressed as  $m$  enhances.



**Fig. 3.** Distribution profiles with different  $M$  in contrast to  $\eta$  (a) velocity profile (b) temperature profile



**Fig. 4.** Distribution profiles with different  $m$  in contrast to  $\eta$  (a) velocity profile (b) temperature profile

The influence of the heat source/sink parameter  $H$  in the present problem is displayed in Figure 5. Figure 5(a) shows the variations of  $-\theta'(0)$  for different values of  $H$  where  $H = 1.0, 2.0, 3.0$  and the dimensionless temperature profile  $\theta(\eta)$  is displayed in Figure 5(b). We noticed that  $H$  has a remarkable impact on the temperature of the  $\text{Al}_2\text{O}_3 - \text{Cu}/\text{H}_2\text{O}$ . Physically,  $-\theta'(0)$  diminishes when the heat generation is incremented due to the presence of additional heat provided in the working flow, hence slow down the heat transmission of the system. This is because more heat is generated and released to the flow, which benefits in enhancing the momentum boundary layer thickness. On another note, the temperature of the hybrid nanofluids  $\theta(\eta)$  rises as a result of the thermal diffusion layer that formed when heat is generated, and this ensues in conjunction with a decrease in the thermal rate. Table 4 demonstrates the results of stability analysis to test the reliability of the solutions. When  $e^{-\Omega\Phi} \rightarrow 0$  as  $\Phi \rightarrow \infty$ , it is recorded that  $\Omega$  generates positive eigenvalues. Meanwhile,  $e^{-\Omega\Phi} \rightarrow \infty$  is recorded to be negative eigenvalues. These findings suggest that the first solution is long-term stable, whereas the second solution is unstable and therefore not long-term physically dependable.

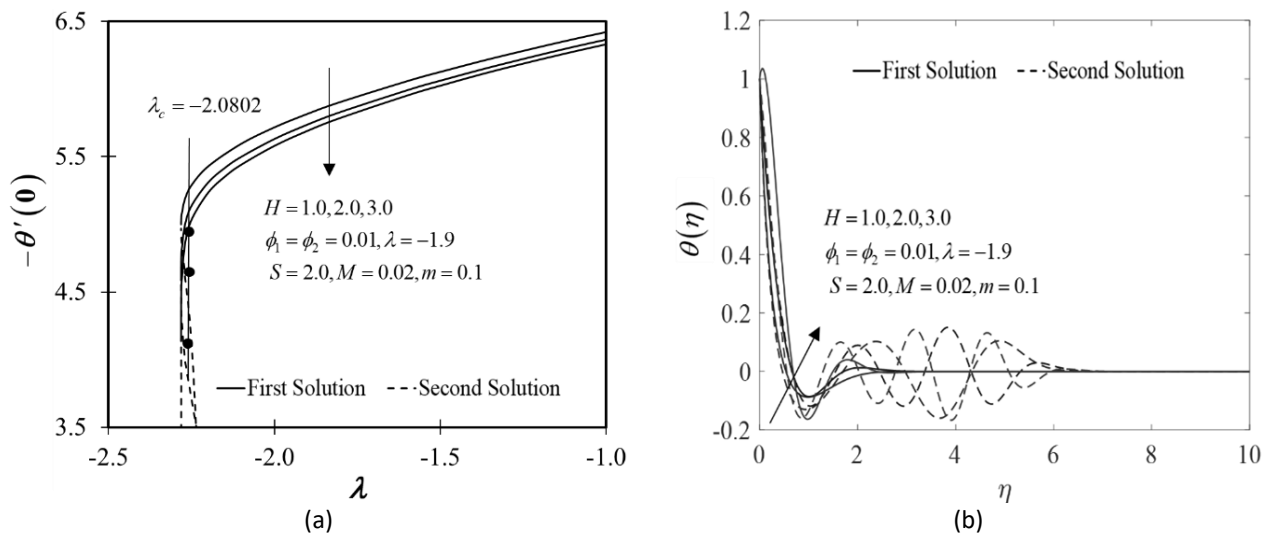


Fig. 5. Different values of  $H$  with  $\lambda$  and  $\eta$  (a) reduced heat transfer coefficient (b) temperature profile

**Table 4**

Results of the smallest eigenvalues  $\Omega$  generated from the analysis of solution stability

$\lambda$	First Solution	Second Solution
-2.0	0.2571	-0.2343
-2.02	0.2192	-0.2172
-2.04	0.1756	-0.1947
-2.06	0.1211	-0.1617
-2.08	0.0131	-0.0781
-2.0802	0.0019	-0.0106

## 5. Conclusions

The recent study verified a numerical simulation of  $\text{Al}_2\text{O}_3\text{-Cu}/\text{H}_2\text{O}$  hybrid nanofluid's response to heat source/sink impact along a shrinking wedge with the addition of several governing parameters. According to the observations, the presence of the first and second solutions is demonstrated for a wide range of control parameters throughout several combinations of the nanoparticle. Through the stability analysis, the first solution has been demonstrated to be in a stable state, while the second solution responds the opposite way.

## Acknowledgement

The authors would like to acknowledge Universiti Teknikal Malaysia Melaka (UTeM) for the financial and technical support under the *Geran Insentif Penerbitan Jurnal 2020* (JURNAL/2020/FTKMP/Q00051).

## References

- [1] Waini, Iskandar, Anuar Ishak, and Ioan Pop. "MHD flow and heat transfer of a hybrid nanofluid past a permeable stretching/shrinking wedge." *Applied Mathematics and Mechanics* 41, no. 3 (2020): 507-520. <https://doi.org/10.1007/s10483-020-2584-7>
- [2] Dinarvand, Saeed, Mohammadreza Nademi Rostami, and Ioan Pop. "A novel hybridity model for  $\text{TiO}_2\text{-CuO}/\text{water}$  hybrid nanofluid flow over a static/moving wedge or corner." *Scientific Reports* 9, no. 1 (2019): 16290. <https://doi.org/10.1038/s41598-019-52720-6>
- [3] Zainal, Nurul Amira, Roslinda Nazar, Kohilavani Naganthran, and Ioan Pop. "Flow and heat transfer over a permeable moving wedge in a hybrid nanofluid with activation energy and binary chemical reaction." *International*

- Journal of Numerical Methods for Heat & Fluid Flow* 32, no. 5 (2022): 1686-1705. <https://doi.org/10.1108/HFF-04-2021-0298>
- [4] Rehman, Rabia, Umar Khan, Hafiz Abdul Wahab, and Basharat Ullah. "Second law analysis for the flow of hybrid nanofluid over a wedge." *Waves in Random and Complex Media* (2022): 1-16. <https://doi.org/10.1080/17455030.2022.2155726>
- [5] Sajjad, Muhammad, Ali Mujtaba, Adnan Asghar, and Teh Yuan Ying. "Dual solutions of magnetohydrodynamics  $Al_2O_3+Cu$  hybrid nanofluid over a vertical exponentially shrinking sheet by presences of joule heating and thermal slip condition." *CFD Letters* 14, no. 8 (2022): 100-115. <https://doi.org/10.37934/cfdl.14.8.100115>
- [6] Idris, Muhammad Syafiq, Irnie Azlin Zakaria, and Wan Azmi Wan Hamzah. "Heat transfer and pressure drop of water based hybrid  $Al_2O_3: SiO_2$  nanofluids in cooling plate of PEMFC." *Journal of Advanced Research in Numerical Heat Transfer* 4, no. 1 (2021): 1-13.
- [7] Manohar, G. R., P. Venkatesh, B. J. Gireesha, J. K. Madhukesh, and G. K. Ramesh. "Dynamics of hybrid nanofluid through a semi spherical porous fin with internal heat generation." *Partial Differential Equations in Applied Mathematics* 4 (2021): 100150. <https://doi.org/10.1016/j.padiff.2021.100150>
- [8] Masood, Sadaf, Muhammad Farooq, and Aisha Anjum. "Influence of heat generation/absorption and stagnation point on polystyrene- $TiO_2/H_2O$  hybrid nanofluid flow." *Scientific Reports* 11, no. 1 (2021): 22381. <https://doi.org/10.1038/s41598-021-01747-9>
- [9] Zainal, Nurul Amira, Roslinda Nazar, Kohilavani Naganthran, and Ioan Pop. "Heat generation/absorption effect on MHD flow of hybrid nanofluid over bidirectional exponential stretching/shrinking sheet." *Chinese Journal of Physics* 69 (2021): 118-133. <https://doi.org/10.1016/j.cjph.2020.12.002>
- [10] Asghar, Adnan, Abdul Fattah Chandio, Zahir Shah, Narcisa Vrinceanu, Wejdan Deebani, Meshal Shutaywi, and Liaquat Ali Lund. "Magnetized mixed convection hybrid nanofluid with effect of heat generation/absorption and velocity slip condition." *Heliyon* 9, no. 2 (2023). <https://doi.org/10.1016/j.heliyon.2023.e13189>
- [11] Chamkha, Ali Javad, Taher Armaghani, Mohamed Ahmed Mansour, Ahmed Mohamed Rashad, and Hadi Kargarsharifabad. "MHD convection of an  $Al_2O_3-Cu$ /water hybrid nanofluid in an inclined porous cavity with internal heat generation/absorption." *Iranian Journal of Chemistry and Chemical Engineering* 41, no. 3 (2022): 936-956.
- [12] Awaludin, Izyan Syazana, Anuar Ishak, and Ioan Pop. "On the stability of MHD boundary layer flow over a stretching/shrinking wedge." *Scientific Reports* 8, no. 1 (2018): 13622. <https://doi.org/10.1038/s41598-018-31777-9>
- [13] Tiwari, Raj Kamal, and Manab Kumar Das. "Heat transfer augmentation in a two-sided lid-driven differentially heated square cavity utilizing nanofluids." *International Journal of Heat and Mass Transfer* 50, no. 9-10 (2007): 2002-2018. <https://doi.org/10.1016/j.ijheatmasstransfer.2006.09.034>
- [14] Oztop, Hakan F., and Eiyad Abu-Nada. "Numerical study of natural convection in partially heated rectangular enclosures filled with nanofluids." *International Journal of Heat and Fluid Flow* 29, no. 5 (2008): 1326-1336. <https://doi.org/10.1016/j.ijheatfluidflow.2008.04.009>
- [15] Raza, Jawad, Azizah Mohd Rohni, and Zurni Omar. "Numerical investigation of copper-water (Cu-water) nanofluid with different shapes of nanoparticles in a channel with stretching wall: Slip effects." *Mathematical and Computational Applications* 21, no. 4 (2016): 43. <https://doi.org/10.3390/mca21040043>
- [16] Weidman, P. D., D. G. Kubitschek, and A. M. J. Davis. "The effect of transpiration on self-similar boundary layer flow over moving surfaces." *International Journal of Engineering Science* 44, no. 11-12 (2006): 730-737. <https://doi.org/10.1016/j.ijengsci.2006.04.005>
- [17] Harris, S. D., D. B. Ingham, and I. Pop. "Mixed convection boundary-layer flow near the stagnation point on a vertical surface in a porous medium: Brinkman model with slip." *Transport in Porous Media* 77 (2009): 267-285. <https://doi.org/10.1007/s11242-008-9309-6>
- [18] Merkin, J. H. "On dual solutions occurring in mixed convection in a porous medium." *Journal of Engineering Mathematics* 20, no. 2 (1986): 171-179. <https://doi.org/10.1007/BF00042775>
- [19] Sparrow, E. M., E. R. G. Eckert, and W. J. Minkowycz. "Transpiration cooling in a magneto-hydrodynamic stagnation-point flow." *Applied Scientific Research, Section A* 11 (1963): 125-147. <https://doi.org/10.1007/BF03184718>
- [20] Ishak, Anuar, Roslinda Nazar, and Ioan Pop. "Falkner-Skan equation for flow past a moving wedge with suction or injection." *Journal of Applied Mathematics and Computing* 25, no. 1-2 (2007): 67-83. <https://doi.org/10.1007/BF02832339>